

# A note about density staircases in the Gulf of Naples : 20 years of persistent weak salt-fingering layers in a coastal area

Florian Kokoszka<sup>1</sup>, Daniele Iudicone<sup>1</sup>, Adriana Zingone<sup>1</sup>, Vincenzo Saggiomo<sup>1</sup>, Maurizio Ribera D'Alcalá<sup>1</sup>, and Fabio Conversano<sup>1</sup>

<sup>1</sup>Stazione Zoologica Anton Dohrn

November 28, 2022

## Abstract

This is a short communication about the inter-annual recurring presence at the coastal site in the Gulf of Naples of density staircases visible below the mixed surface layer of the water-column, from the end of summer to the beginning of winter, each year during nearly two decades of survey (2001 to 2020). We repetitively observe sequences from 1 to 4 small vertical staircases structures ( $\sim 3$  m thick) in the density profiles ( $\sim \Delta 0.2$  kg/m<sup>3</sup>), located between 10 m to 50 m deep below the seasonal mixed layer depth. We interpret these vertical structures as the result of double diffusive processes that could host salt-fingering regime (SF) due to warm salty water parcels overlying on relatively fresher and colder layers. This common feature of the Mediterranean basin (i.e., the thermohaline staircases of the Tyrrhenian sea) may sign here for the lateral intrusions of nearshore water masses. These stably stratified layers are characterized by density ratio  $R_\rho$  5.0 to 10.0, slightly higher than the critical range (1.0 - 3.0) generally expected for fully developed salt-fingers. SF mixing, such as parameterized (Zhang et al., 1998), appears to inhibit weakly the effective eddy diffusivity with negative averaged value ( $\sim -1e-8$  m<sup>2</sup>/s). A quasi 5-year cycle is visible in the inter-annual variability of the eddy diffusivity associated to SF, suggesting a decadal modulation of the parameters regulating the SF regime. Even contributing weakly to the turbulent mixing of the area, we hypothesis that SF could influence the seasonal stratification by intensifying the density of deep layers. Downward transfer of salt could have an impact on the nutrient supply for the biological communities, that remains to be determined.

1 A note about density staircases in the Gulf of  
2 Naples : 20 years of persistent weak salt-fingering  
3 layers in a coastal area

4 Florian Kokoszka\*, Daniele Iudicone\*,  
Adriana Zingone\*, Vincenzo Saggiomo\*,  
Maurizio Ribera d'Alcalá\*, and Fabio Conversano\*

5 \* *Stazione Zoologica Anton Dohrn, Naples, Italy*

6 Corresponding author: Florian Kokoszka  
7 `florian.kokoszka@szn.it`

8 July 2021

9 Keywords

10 Coastal ecosystem, Mediterranean sea, time series, hydrological data, turbu-  
11 lence, stratification, mixing, double-diffusion, salt-fingers

12 List of Figures

- 13
- 14 • Fig. 1 : Location and bathymetry of the Gulf of Naples in the Mediter-  
15 ranean basin.
  - 16 • Fig. 2 : Mean climatological seasonal cycle of the water-column occupa-  
17 tion by the double-diffusive regime, and illustration of the density stair-  
18 cases with an in-situ example.
  - 19 • Fig. 3 : Time series (2001-2020) of the vertical profiles of the density ratio  
20 and the parameterized effective eddy diffusivity.
  - 21 • Fig. 4 : Statistical distributions and inter-annual variability of the salt-  
22 fingering parameters.

## 23 Abstract

24 This is a short communication about the inter-annual recurring presence at the  
25 coastal site in the Gulf of Naples of density staircases visible below the mixed  
26 surface layer of the water-column, from the end of summer to the beginning of  
27 winter, each year during nearly two decades of survey (2001 to 2020). We repet-  
28 itively observe sequences from 1 to 4 small vertical staircases structures ( $\sim 3$  m  
29 thick) in the density profiles ( $\sim \Delta 0.2 \text{ kg m}^{-3}$ ), located between 10 m to 50 m  
30 deep below the seasonal mixed layer depth. We interpret these vertical struc-  
31 tures as the result of double diffusive processes that could host salt-fingering  
32 regime (SF) due to warm salty water parcels overlying on relatively fresher  
33 and colder layers. This common feature of the Mediterranean basin (i.e., the  
34 thermohaline staircases of the Tyrrhenian sea) may sign here for the lateral  
35 intrusions of nearshore water masses. These stably stratified layers are char-  
36 acterized by density ratio  $R_\rho$  from 5.0 to 10.0, slightly higher than the critical  
37 range (1.0 – 3.0) generally expected for fully developed salt-fingers. SF mixing,  
38 such as parameterized (Zhang et al. (1998)), appears to inhibit weakly the ef-  
39 fective eddy diffusivity with negative averaged value ( $\sim -1 \times 10^{-8} \text{ m}^2 \text{ s}^{-1}$ ). A  
40 quasi 5-year cycle is visible in the inter-annual variability of  $\langle K^{\text{SF}} \rangle$ , suggest-  
41 ing a decadal modulation of the parameters regulating the SF regime. Even  
42 contributing weakly to the turbulent mixing of the area, we hypothesize that  
43 SF could influence the seasonal stratification by intensifying the density of deep  
44 layers. Downward transfer of salt could have an impact on the nutrient supply  
45 for the biological communities, that remains to be determined.

## 46 1 Introduction

47 Double diffusive mixing in the ocean is driven by the difference between molec-  
48 ular diffusivities of heat and salt (Stommel et al., 1956), the diffusion of heat  
49 being roughly 100 times faster than for salt (Zhang et al., 1998). This can  
50 be illustrated by the case of relatively warm water parcels that stabilize lo-  
51 cally the water-column, tending to rapidly diffuse their heat content, while the  
52 slower diffusion of the salty content renders the vertical stability prompt to  
53 gravitational collapse. This situation leads to a transfer of salt toward the bot-  
54 tom, denominated as salt-fingering (SF) after their famously known chimney  
55 structure (Stommel et al., 1956; Stern, 1960; Linden, 1973). Another situation  
56 can occur too, when relatively cold and fresh water overlays on warmer and  
57 saltier parcels. Thermal content diffusion tends to stabilize upward, bringing  
58 salty parcels toward the surface, and an oscillatory diffusive (DDF) instability  
59 is generated. Once established in the water-column, these diffusive regimes can  
60 be identified in the vertical profiles of density by a series of well-mixed layers,  
61 whose staircases signature can extend from relatively vertical thin or fine-scale  
62 layers (e.g., 5 to 100-m thick intrusions, Ruddick, Richards (2003)) to larger  
63 structures (e.g. 300-m thick in the Tyrrhenian sea in Durante et al. (2019))  
64 This process has been widely observed since decades in the ocean (e.g., Schmitt  
65 et al. (2005) in the Atlantic Ocean, Timmermans et al. (2003) and Lenn et al.  
66 (2009) in the Arctic), and particularly in the Mediterranean sea (Meccia et al.,  
67 2016; Falco, 2016), but field observations and time series acquisition remain of  
68 importance to investigate properly the temporal variability associated to these  
69 diffusive phenomena, as pointed out by the study of Durante et al. (2019).  
70 Weak turbulent environment remains a key condition for their establishment  
71 against strong mixing processes (Timmermans et al., 2003), but the compi-  
72 lation of all in-situ observations demonstrates decades of their persistence in  
73 the Mediterranean basin with spatially distributed coherent patterns (Buffett  
74 et al., 2017). Even their turbulent mixing has been shown to contribute weakly  
75 to the ocean circulation (Lenn et al., 2009; Boog et al., 2021), their influence  
76 to the buoyancy flux can be significant in non-sheared environment and should  
77 be taken in account properly in the water-column budgets (Inoue et al., 2007).  
78 Due to the direct transfer of salt they provide toward the deep layers, and even  
79 weakly turbulent, double diffusive processes are effective and of importance to  
80 supply nutrients for the biological activity in the internal part of the water col-  
81 umn (Fernández Castro et al., 2015)). Historically, studies of this phenomenon  
82 focused on the open and interior part of the ocean basins, but lakes, shallow  
83 seas and coastal area can be concerned too (Carniel et al., 2008; Schmid et al.,  
84 2010; Umlauf et al., 2018). Coastal marine ecosystem such as the Gulf of Naples  
85 is a mid-latitude semi-enclosed shallow basin in the Western Mediterrean Sea  
86 having a subtropical regime and almost no tides (**Fig. 1**). The area presents  
87 a marked salinity contrast due to the combination of the salty Tyrrhenian Sea  
88 waters, with its own feature of inshore/offshore water exchange with the open  
89 ocean, located on its southern side (Cianelli et al., 2015), and the freshwater  
90 inputs from a densely inhabited coastal area, on its northern part and from

91 nearby rivers (Cianelli et al., 2012, 2017).

92 The recent study of Kokoszka et al. (2021) in this location shows weak tur-  
93 bulent observations during the seasonal destratification, associated to the pres-  
94 ence of double-diffusive layers below the intrusion of warm salty layers present  
95 in sub-surface from late summer to early winter. We extend this half-year pe-  
96 riod analysis to the long-term time series in the Gulf of Naples with the use of  
97 temperature and salinity profiles. These observations were made in the frame-  
98 work of the Long Term Ecosystem Research Marechiarà (LTER-MC) initiative  
99 that produced a historical time series of the mediterranean coastal ecosystem  
100 of the Gulf of Naples through a weekly sampling of the water column started in  
101 1984 and running until now (Ribera d'Alcalá et al., 2004; Zingone et al., 2019).  
102 We will focus here on the two last decades (January 2001 to March 2020), and  
103 identify the layers of the water-column prompt to salt-finger regimes, to show  
104 their variability, and estimate the associated eddy diffusivity, to determine their  
105 possible contribution to the vertical mixing in such coastal area.

## 106 2 Materials and Methods

### 107 *General hydrology*

108 Conductivity–Temperature–Depth (CTD) profiles were carried out at the  
109 LTER-MC sampling point in the Gulf of Naples (**Fig. 1**) with a Seabird  
110 SBE-911+ mounted on a 12-bottle carousel, with all sensors calibrated. The  
111 raw profiles were processed using the Seabird data processing software to obtain  
112 1-m bin-averaged data. The weekly survey refers to the casts MC465 (January  
113 2001) to MC1359 (February 2020) and includes a total of 895 CTD profiles.  
114 The Gibbs-SeaWater Oceanographic Toolbox (McDougall, Barker, 2011) was  
115 used to calculate the conservative temperature  $\Theta$  ( $^{\circ}\text{C}$ ), the absolute salinity  
116  $A_S$  ( $\text{g kg}^{-1}$ ), the potential density  $\sigma_0$  ( $\text{kg m}^{-3}$ ), and the potential temperature  
117  $\theta_0$  ( $^{\circ}\text{C}$ ). When mentioned thereafter, temperature  $T$  and salinity  $S$  refer to  $\Theta$   
118 and  $A_S$ . Mixed layer depth (MLD, m) was calculated following the method of  
119 Boyer Montégut de et al. (2004) based on threshold values. Given a vertical  
120 profile of density  $\sigma_0(z)$ , we calculated the depth below  $z_{\text{ref}} = 3\text{m}$  where the  
121 profile reached a threshold defined as a cumulative of  $0.03 \text{ kg m}^{-3}$ .

### 122 *Turner’s stability regimes*

123 To produce reliable statistics of the double diffusive regimes, we followed  
124 the recommendation of Inoue et al. (2007) that compared successfully CTD  
125 estimates and dedicated turbulence measurements. We applied the same 10-  
126 m-scale averaging on temperature and salinity profiles, and conserved only the  
127 parts of the water column where the threshold for the minimum temperature  
128 gradient was  $|\partial\bar{\theta}/\partial z| > 0.05 \text{ }^{\circ}\text{C m}^{-1}$  (Zhang et al., 1998; Inoue et al., 2007). This  
129 was shown to improve the statistics by embedding the information contained  
130 in the layer, that determines then the processes occurring at finer scales (Inoue  
131 et al., 2007). We applied the method introduced by Turner (Turner, 1967; 1973)  
132 to localize parts of the water column where vertical gradients of  $T$  and  $S$  are  
133 favourable to double-diffusive instability. Combining the vertical gradients and  
134 their signs allows the identification of stability regimes, that can be defined  
135 from the density ratio  $R_\rho = (\alpha\partial\theta/\partial z)/(\beta\partial S/\partial z)$  where  $\alpha = -\rho^{-1}(\partial\rho/\partial\theta)$  is  
136 the thermal expansion coefficient,  $\beta = \rho^{-1}(\partial\rho/\partial S)$  is the haline contraction  
137 coefficient, where  $\partial\rho/\partial z$  and  $\partial\theta/\partial z$  are the vertical gradients of density and  
138 temperature, respectively. This ratio is used to calculate the Turner angles ( $^{\circ}$ )  
139  $Tu = \arctan((1 + R_\rho)/(1 - R_\rho))$  (Ruddick, 1983). The value of the Turner  
140 angle allows to identify various stability regimes. A diffusive convection regime  
141 (e.g., fresh cold layers over warm salty layer) arises when  $-90^{\circ} < Tu < -45^{\circ}$ .  
142 A double-diffusive regime (e.g., salty warm layer over cold fresh layer) arises  
143 when  $45^{\circ} < Tu < 90^{\circ}$ . Within each of these regimes, the instability is higher  
144 when  $|Tu|$  is close to 90 degrees. A stable regime occurs when  $|Tu| < 45^{\circ}$ ,  
145 whereas a gravitationally unstable regime occurs when  $|Tu| > 90^{\circ}$ . Generally,  
146 salt-fingering is considered active when  $1 < R_\rho < 3$  (Inoue et al., 2007; Carniel

147 et al., 2008), but as illustrated thereafter on the **Fig. 2**, our observations  
 148 exhibit small density staircases ( $\sim 3$  m) associated to slightly larger values of  
 149  $R_\rho$  (3.0 – 5.0), that should sign for a weak salt-fingering regime, but marked by  
 150 persisting structures, visible repetitively weeks after weeks. Given that values  
 151  $1 < R_\rho < 10$  are frequently observed (Kelley, 1990), and the large variability  
 152 of the worldwide observations (You, 2002; Nakano, Yoshida, 2019), we included  
 153 then all the cases  $1 < R_\rho < 30$ .

#### 154 *Salt-fingering diffusivities and salty flux*

155 From the estimates of  $R_\rho$ , diffusivities of heat, salt, and density associated  
 156 with salt-fingering have been extensively reviewed and are still discussed un-  
 157 til now (Kunze, 2003; Nakano, Yoshida, 2019). Once identified parts of the  
 158 water column prompt to SF regime, we apply the parameterization of Zhang  
 159 et al. (1998) to obtain the effective salt and thermal diffusivities, respectively  
 160  $K_S^{\text{SF}} = K^*/(1 + (R_\rho/R_C)^n)$  and  $K_T^{\text{SF}} = \gamma^{\text{SF}}(K_S^{\text{SF}})/R_\rho$ , where  $n = 6$ ,  $R_C = 1.6$ ,  
 161  $K^* = 1 \times 10^{-4} \text{ m}^2 \text{ s}^{-1}$  a upper limit for the SF diffusivity, and  $\gamma^{\text{SF}}$  is computed  
 162 as  $\gamma^{\text{SF}} = 2.709e^{-2.512R_\rho} + 0.5128$  (Radko, Smith, 2012). Finally, we infer the ef-  
 163 fective eddy diffusivity of the density,  $K_\rho^{\text{SF}} = (K_T^{\text{SF}} R_\rho - K_S^{\text{SF}})/(R_\rho - 1)$  (Eq. 8 in  
 164 Nakano, Yoshida (2019)). As pointed out by the authors in their review, values  
 165 of  $K_\rho^{\text{SF}}$  are negative, indicating that SF reduces the potential energy of the sys-  
 166 tem by transferring salt downward in the water-column, and consequently inten-  
 167 sifies density stratification. To illustrate that, we recall a general expression for  
 168 the diffusivity (valid for heat, salt, or density) as a combination of salt-fingering  
 169 (SF), double-diffusive (DDF), and other processes than double-diffusion (e.g.,  
 170 internal wave turbulence):  $K^{\text{TOTAL}} = K^{\text{Turb.}} + K^{\text{SF}} + K^{\text{DDF}}$  (Merryfield et al.,  
 171 1999; Merryfield, 2000; Inoue et al., 2007);  $K^{\text{TOTAL}}$  is generally dominated by  
 172 the contribution of  $K^{\text{Turb.}}$ , and can be reduced by the negative values of  $K^{\text{SF}}$ .  
 173 Please note that double-diffusive (DDF) will not be discussed in this work, and  
 174 has been reviewed in detail by the mentioned authors. An estimate of buoyancy  
 175 flux for salt is given by Kunze (1987) for SF developed on "thick" layers ( $> 1$  m),  
 176 as  $g\beta F_S = 2\nu g\beta(\partial\bar{S}/\partial z)(R_\rho^{1/2} + (R_\rho - 1)^{1/2})^2$  (Kunze (1987), and Eq. 97 in  
 177 Nakano, Yoshida (2019)), with  $g$  the gravitational acceleration ( $9.80 \text{ m s}^{-2}$ ),  $\nu$   
 178 the kinematic molecular viscosity ( $1.05 \times 10^{-6} \text{ m}^2 \text{ s}^{-1}$ ). Here  $F_S$  is the vertical  
 179 salt flux ( $\text{g kg}^{-1} \text{ m s}^{-1}$ ),  $\beta F_S$  the density flux of salt ( $\text{m s}^{-1}$ ), and  $g\beta F_S$  the  
 180 buoyancy flux ( $\text{m}^2 \text{ s}^{-3}$ ).

181 **2.1 Results**

182 *Staircases layers during the seasonal cycle*

183 Established from the weekly profiles of the whole period 2001-2020, the cli-  
184 matological monthly variations of salinity show a remarkable intrusion in sub-  
185 surface (thick blue contour on **Fig. 2, top**), with values close to the maxi-  
186 mum, between  $38.05$  and  $38.1 \text{ g kg}^{-1}$ , visible from September to November be-  
187 low  $10 \text{ m}$  depth, and above the  $20 \text{ m}$  to  $45 \text{ m}$  layer of relative less salty water ( $<$   
188  $38.0 \text{ g kg}^{-1}$ ). The thickness of this salty tongue increases in time following the  
189 deepening of the seasonal thermocline up to November (MLD in thick gray line  
190 on **Fig. 2, top**), progressively filling the water column, besides the first  $5 \text{ m}$ .  
191 Temperature (black contours on **Fig. 2, top**) shows a more classical seasonal  
192 cycle, with a mean maximum of around  $26^\circ\text{C}$  in July and August, decreasing  
193 to  $20.0^\circ\text{C}$  in September, then to  $24.0^\circ\text{C}$  and  $18.0^\circ\text{C}$  in October and November.  
194 From August to November these intrusions of salty water from  $10$  to  $60 \text{ m}$  create  
195 the unstable conditions for SF regime, whose water-column occupation is shown  
196 in plain blue on **Fig. 2 (top)**, below the MLD (thick gray).

197 The overview of the mean seasonal hydrological state allowed us to identify  
198 some general vertical distribution of SF regimes during the seasonal cycle. We  
199 illustrate this situation by showing a typical example of small staircases (e.g.,  
200 during the cast MC1126 on **Fig. 2, bottom**). From around  $25$  to  $45 \text{ m}$  deep,  
201 both gradients of  $T$  and  $S$  are compatible with the host of SF regime. A sharp  
202 variation of nearly  $0.2 \text{ g kg}^{-1}$  is visible between  $30$  and  $32 \text{ m}$ , followed by a more  
203 moderate one of  $0.1 \text{ g kg}^{-1}$  from  $32$  to  $37 \text{ m}$ , associated both with a loss of  
204 temperature of nearly  $1.0^\circ\text{C}$ . The density profile is then marked by a sequence  
205 of thin and curvy staircases, progressing stably toward depth by steps of  $\sim$   
206  $0.20 \text{ kg m}^{-3}$  on vertical scales from  $1$  to  $3 \text{ m}$ . In terms of Turner angles, stronger  
207 value of  $60^\circ$  is obtained at  $27 \text{ m}$  where the instability presumably initiates from  
208 the salty and warm input, and progressively decreases to around  $50^\circ$  at  $40 \text{ m}$   
209 where  $T - S$  gradients stop to host the SF regime. Associated values of  $R_\rho$  vary  
210 from  $3.0$  to  $5.0$  where density staircases are the sharpest, then increase above  
211  $10.0$  at the host ending. These values are slightly above the range in which  
212 SF are expected to be the most active ( $1.0 - 3.0$ ), but density observations are  
213 marked by small curvy staircases, whose vertical structure have been smoothed  
214 by the  $1\text{-m}$  scale vertical averaging of the data. Given these values of  $R_\rho$  and  
215 the shape of density profiles, we consider that we observe here a relatively weak  
216 SF regime, and this situation tends to repeat and persist in time during the  
217 season.

218 *Unfolding the layers : nearly 20 years of staircase layers*

219 This persistence during the two last decades is clearly demonstrated on the  
220 **Fig. 3** with the vertical distribution of  $R_\rho$  showing the vertical hosting of the  
221 SF regime below the mean MLD (gray line), mainly from August to Novem-  
222 ber. Even being weak in general ( $Tu$  in the range  $45 - 60^\circ$ ), the most intense

223 Turner angles values are more frequent in October and November than during  
 224 the summer (see the vertical patterns on **Fig. 3**, and the red to blue distribu-  
 225 tions on **Fig. 4**). Mean values of  $R_\rho$  are between 5.0 and 10.0, and occurrences  
 226  $< 5.0$  are more frequent in October and November. Estimates of salt and  
 227 thermal diffusivities reach mean values centered around  $1 \times 10^{-8} \text{ m}^2 \text{ s}^{-1}$  and  
 228  $4 \times 10^{-9} \text{ m}^2 \text{ s}^{-1}$  during these months, while the intensity is weaker and close to  
 229  $1 \times 10^{-11} \text{ m}^2 \text{ s}^{-1}$  in August. This marks a seasonal differentiation in our obser-  
 230 vations, the post-summer period being prompter to host the more intense SF  
 231 regimes. When estimating the effective eddy diffusivity for the density, values of  
 232  $K_\rho^{\text{SF}}$  are negative, indicating that SF reduces the potential energy of the system  
 233 by transferring salt downward in the water-column. Mean contribution is low  
 234 ( $-3 \times 10^{-8} \text{ m}^2 \text{ s}^{-1}$ ), compared to the averaged turbulent diffusivity expected in  
 235 such coastal system (from  $1 \times 10^{-6} \text{ m}^2 \text{ s}^{-1}$  to  $1 \times 10^{-4} \text{ m}^2 \text{ s}^{-1}$ ). The range of  
 236 the associated buoyancy flux for salt is around  $-6 \times 10^{-9} \text{ m}^2 \text{ s}^{-3}$  from Septem-  
 237 ber to October (see the yellow, orange and blue distributions on **Fig. 4**), and  
 238 is centered closer to  $-1 \times 10^{-8} \text{ m}^2 \text{ s}^{-3}$  in August (red). Consequently SF mix-  
 239 ing, such as parameterized, appears to inhibit weakly the turbulent mixing of  
 240 the area ( $K^{\text{TOTAL}} = K^{\text{Turb.}} + K^{\text{SF}} + K^{\text{DDF}}$ ), but increase the stability of the  
 241 deep layers by intensifying the density stratification due to the transfer of salt  
 242 toward the bottom. The inter-annual values (black plots on **Fig. 4**) of  $K_\rho$   
 243 confirms these averages ranging from  $-1 \times 10^{-10} \text{ m}^2 \text{ s}^{-1}$  to  $-1 \times 10^{-6} \text{ m}^2 \text{ s}^{-1}$ ,  
 244 and the low averaged buoyancy flux for salt ( $\sim -6 \times 10^{-9} \text{ m}^2 \text{ s}^{-3}$ ) compared to  
 245 the expected total buoyancy fluxes due to heat and freshwater by atmospheric  
 246 forcings at the surface (of the order of  $\sim 1 \times 10^{-7} \text{ m}^2 \text{ s}^{-3}$ , see Kokoszka et al.  
 247 (2021)). Noteworthy, a quasi 5-year cycle modulation is visible, affecting the  
 248 transition of the first decade (2000-2009) to the second one (2010-2019), marked  
 249 by weaker values for  $K_\rho$ . If these SF layers are the results of warm and salty  
 250 intrusions, this suggest the presence of a climatic mechanism able to modulate  
 251 the inter-annual variability inshore-offshore advection of such features at the  
 252 time scale of the decade.

## 253 2.2 Discussion

254 The long-term monitoring (20 years) of the coastal station Marechiarra in the  
255 Gulf of Naples (LTER-MC, 75 m deep, 2 km off the coast) reveals noteworthy  
256 repetitive observations of small staircases vertical structures ( $\sim 3$  m) in the  
257 density field ( $\sim \Delta 0.2 \text{ kg m}^{-3}$ ), whose presence is associated to surrounding layers  
258 of relatively warm and salty waters in sub-surface (from 10 to 50 m deep) from  
259 August to November, each year. We interpret these observations as the result  
260 of double-diffusive processes, i.e. here salt-fingering instabilities.

261 Such fine-scale structures may sign here for lateral intrusions (Merryfield,  
262 2000; Umlauf et al., 2018), or interleaving (Ruddick, Richards, 2003; Ruddick,  
263 Kerr, 2003), whose inshore advection remains to be determined. These stably  
264 stratified layers are characterized by density ratio  $R_\rho$  from 5.0 to 10.0, close to  
265 some observations made in the Arctic Ocean (Timmermans et al., 2008; Shibley  
266 et al., 2017). As pointed out by Bebieva, Timmermans (2017), taking in account  
267 the horizontal gradients of T and S (intrusions), a critical value for the insta-  
268 bility does not necessarily need to be close to 1.0, the higher values of  $R_\rho$  being  
269 the signature of T-S intrusions. This may be what we observe here, differing  
270 from the T-S staircases, typical of the neighbouring Tyrrhenian Sea (Zodiatis,  
271 Gasparini, 1996; Durante et al., 2019). In such configuration, dedicated param-  
272 eterization taking account of horizontal gradients and using intermediate and  
273 higher  $R_\rho$  values should be investigated.

274 Given the averaged values of  $R_\rho$  ( $\sim 5.0$ ) and the observed values of turbu-  
275 lent mixing ( $\langle K^{\text{Turb}} \rangle$  between  $0.2$  to  $0.8 \times 10^{-5} \text{ m}^2 \text{ s}^{-1}$ , in Kokoszka et al.  
276 (2021)), the inhibition due to negative  $\langle K^{\text{SF}} \rangle$  in the *mixing mixture* (In-  
277 oue et al., 2007) is expected to be negligible, even some intermittent unstable  
278 occurrences ( $R_\rho$  close to 1.0) can be present in the SF layer below the MLD.  
279 Even mixing would be unaffected, the density stratification enforcement due  
280 to the transfer of salt could influence the generation and propagation of in-  
281 ternal waves in such stratified-compatible layers (Kunze, 2003; Malki-Epshtein,  
282 Huppert, 2004; Maurer, Linden, 2014), followed then by their breaking in the  
283 deepest layers, more relaxed to the buoyancy-control of vertical motions. When  
284 the SF-compatible layers are located closer to the bottom (e.g., around 50 m  
285 in November), influence of boundary processes could be at work too, as sug-  
286 gested by the turbidity observations of Kokoszka et al. (2021). The step size  
287 of the observed structures could be a clue of the coexistence between weakly  
288 sheared internal wave and double-diffusion processes, as mentioned in the re-  
289 view of Kunze (2003). This feature of the shallow non-tidal area of the Gulf  
290 of Naples could provide an interesting in-situ experimental field to investigate  
291 and understand better the dynamic behind background gradients of tracers and  
292 velocity, and the growing of SF instabilities (Inoue et al., 2008; Ma, Peltier,  
293 2021).

294 In general, implications for biological communities could be important. Com-  
295 pared to fluxes associated with mechanical forcings or mesoscale eddies, Oschlies  
296 et al. (2003) found the same magnitude attributed to double-diffusive processes,  
297 that showed a salt-finger driven enhancement of the upper ocean nutrient sup-

298 ply. As estimated in the work of Fernández Castro et al. (2015), nitrate diffusion  
299 mediated by salt fingers is responsible for  $\sim 20\%$  of the new nitrogen supply  
300 in several areas of the Atlantic and Indian Oceans. More recently, Taillandier  
301 et al. (2020) showed that the nitrates supply across thermohaline staircases in  
302 the Western Mediterranean sea contributed at 25% to the budget of the Levantine  
303 intermediate water. The Gulf of Naples stands as a shallow bay connected to  
304 the open Tyrrhenian area, and Cianelli et al. (2017) shown here the importance  
305 of the interplay between coastal and offshore water masses to promote phyto-  
306 plankton diversity. Their study identified the role of the horizontal mixing to  
307 enhance or dilute the favourable conditions for dominant species, and under this  
308 hypothesis we propose that salty intrusions (i.e., horizontal gradients), should  
309 be investigated in terms of their stability relative to the vertically surrounding  
310 layers. Given the downward transfer of salt due to SF regime in this shallow  
311 area where the photic layer prevails for the growing dynamic of the biological  
312 populations (Zingone et al., 1995, 2010), the importance of such a supply to the  
313 communities inhabiting the deep layers is a primer to determine. Because SF  
314 activity depends on the density ratio rather than on the stratification stability,  
315 its sensitivity to the future expected warming/freshening trends of the surface  
316 waters in the Mediterranean sea (Volosciuk et al., 2016) should be addressed,  
317 as shown by the inter-annual decadal variability already observable here at the  
318 coastal site in the Gulf of Naples.

## 319 **Acknowledgments**

320 Data sets for this research are available on request. We would like to thank  
321 the LTER-MC team that includes, besides the main authors: D. d’Alelio, C.  
322 Balestra, M. Cannavacciuolo, R. Casotti, I. Di Capua, F. Margiotta, M. G.  
323 Mazzocchi, M. Montresor, A. Passarelli, I. Percopo, M. Ribera d’Alcalà, M.  
324 Saggiomo, V. Saggiomo, D. Sarno, F. Tramontano, G. Zazo, A. Zingone, all  
325 based at the Stazione Zoologica Anton Dohrn of Naples. Special thanks must  
326 be given to A. Passarelli and the commandants and crews of the R/V Vettorica for  
327 all their dedicated work at sea. The research program LTER-MC is supported  
328 by the Stazione Zoologica Anton Dohrn.

## 329 **References**

- 330 Bebieva Yana, Timmermans Mary-Louise. The Relationship between Double-  
331 Diffusive Intrusions and Staircases in the Arctic Ocean // Journal of Physical  
332 Oceanography. 02 2017. 47.
- 333 Boog Carine, Dijkstra Henk, Pietrzak Julie, Katsman Caroline. Double-diffusive  
334 mixing makes a small contribution to the global ocean circulation // Com-  
335 munications Earth Environment. 02 2021. 2. 46.
- 336 Boyer Montégut C. de, Madec G., Fischer A. S., Lazar A., Iudicone D. Mixed  
337 layer depth over the global ocean: An examination of profile data and profile-  
338 based climatology // Journal of Geophysical Research. 01 2004. 109. C12003.
- 339 Buffett Grant George, Krahnemann G., Klaeschen Dirk, Schroeder Katrin,  
340 Sallares Valenti, Papenberg Cord, R. Ranero Cesar, Zitellini Nevio. Seis-  
341 mic Oceanography in the Tyrrhenian Sea – Thermohaline Staircases, Eddies  
342 and Internal Waves // Journal of Geophysical Research: Oceans. 09 2017.  
343 122.
- 344 Carniel Sandro, Sclavo Mauro, Kantha Lakshmi, Prandke Hartmut. Double-  
345 diffusive layers in the Adriatic Sea // Geophysical Research Letters. 01 2008.  
346 35.
- 347 Cianelli Daniela, D’Alelio Domenico, Uttieri Marco, Sarno Diana, Zingone  
348 Adriana, Zambianchi Enrico, Ribera d’Alcala Maurizio. Disentangling phys-  
349 ical and biological drivers of phytoplankton dynamics in a coastal system //  
350 Scientific Reports. 12 2017. 7.
- 351 Cianelli Daniela, Falco Pierpaolo, Iermano Ilaria, Mozzillo Pasquale, Uttieri  
352 Marco, Buonocore B., Zambardino Giovanni, Zambianchi Enrico. In-  
353 shore/offshore water exchange in the Gulf of Naples // Journal of Marine  
354 Systems. 01 2015.
- 355 Cianelli Daniela, Uttieri Marco, Buonocore B., Falco Pierpaolo, Zambardino  
356 Giovanni, Zambianchi Enrico. Dynamics of a very special Mediterranean  
357 coastal area: the Gulf of Naples // Mediterranean Ecosystems: Dynamics,  
358 Management and Conservation. 08 2012. 129–150.
- 359 Durante Sara, Schroeder Katrin, Mazzei L., Pierini S., Borghini M., Sparnocchia  
360 S. Permanent Thermohaline Staircases in the Tyrrhenian Sea // Geophysical  
361 Research Letters. 01 2019.
- 362 Falco Pierpaolo. Water mass structure and deep mixing processes in the Tyrrhe-  
363 nian Sea: Results from the VECTOR project // Deep Sea Research Part I  
364 Oceanographic Research Papers. 04 2016. 113.
- 365 Fernández Castro Bieito, Mourino Beatriz, Maranon Emilio, Chouciño P, Gago  
366 J., Ramírez Teodoro, Vidal Montserrat, Bode Antonio, Blasco D, Royer

367 Sarah-Jeanne, Estrada Marta, Simó Rafel. Importance of salt fingering for  
368 new nitrogen supply in the oligotrophic ocean // Nature communications. 09  
369 2015. 6. 8002.

370 GEBCO Compilation Group. GEBCO 2020 Grid. 2020.

371 Inoue R., Kunze E., Laurent L., Schmitt Raymond, Toole John. Evaluating  
372 salt-fingering theories // Journal of Marine Research. 07 2008. 66.

373 Inoue Ryuichiro, Yamazaki Hidekatsu, Wolk Fabian, Kono Tokihiro, Yoshida  
374 Jiro. An Estimation of Buoyancy Flux for a Mixture of Turbulence and  
375 Double Diffusion // Journal of Physical Oceanography. 03 2007. 37.

376 Kelley Dan. Fluxes Through Diffusive Staircases, A New Formulation // Journal  
377 of Geophysical Research. 03 1990. 95. 3365–3371.

378 Kokoszka Florian, Conversano Fabio, Iudicone Daniele, Ferron Bruno,  
379 Bouruet-Aubertot Pascale, Mc Millan Justine. Microstructure observations  
380 of the summer-to-winter destratification at a coastal site in the Gulf of Naples  
381 // Essoar pre-print. 7 2021.

382 Kunze Eric. Limits on Growing, Finite-Length Salt Fingers, A Richardson  
383 Number Constraint // J. Mar. Res. 08 1987. 45. 533–556.

384 Kunze Eric. A review of oceanic salt-fingering theory // Progress In Oceanog-  
385 raphy. 03 2003. 56. 399–417.

386 Lenn Yueng-Djern, Wiles P.J., Torres-Valdés Sinhué, Abrahamsen Einar,  
387 Rippeth Tom, Simpson John, Bacon S., Laxon S., Polyakov I., Ivanov  
388 Vladimir, Kirillov Sergey. Vertical mixing at intermediate depths in the Arctic  
389 boundary current // Geophysical Research Letters. 03 2009. 36. L05601.

390 Linden P.F. On the Structure of Salt Fingers // Deep Sea Res. 04 1973. 20.  
391 325–340.

392 Ma Yuchen, Peltier W. Gamma instability in an inhomogeneous environment  
393 and salt-fingering staircase trapping: Determining the step size // Physical  
394 Review Fluids. 03 2021. 6.

395 Malki-Epshtein Liora, Huppert Herbert. Internal waves and velocity scales of  
396 double-diffusive intrusions // 57th Annual Meeting of the APS Division of  
397 Fluid Dynamics, 21-23 November, 2004, Seattle, USA. 01 2004.

398 Maurer Benjamin, Linden P. Intrusion-generated waves in a linearly stratified  
399 fluid // Journal of Fluid Mechanics. 08 2014. 752. 282–295.

400 McDougall T.J., Barker P.M. Getting started with TEOS-10 and the Gibbs  
401 Seawater (GSW) Oceanographic Toolbox // SCOR/IAPSO WG. 2011. 127.  
402 1—28.

- 403 Meccia Virna, Simoncelli Simona, Sparnocchia Stefania. Decadal variability of  
404 the Turner Angle in the Mediterranean Sea and its implications for double  
405 diffusion // Deep Sea Research Part I: Oceanographic Research Papers. 08  
406 2016. 114. 64–77.
- 407 Merryfield William. Origin of Thermohaline Staircases // Journal of Physical  
408 Oceanography - J PHYS OCEANOGR. 05 2000. 30. 1046–1068.
- 409 Merryfield William, Holloway Greg, Gargett Ann. A Global Ocean Model with  
410 Double-Diffusive Mixing // Journal of Physical Oceanography - J PHYS  
411 OCEANOGR. 06 1999. 29. 1124–1142.
- 412 Nakano Haruka, Yoshida Jiro. A note on estimating eddy diffusivity for oceanic  
413 double-diffusive convection // Journal of Oceanography. 05 2019.
- 414 Oschlies Andreas, Dietze H., Kähler Paul. Salt-finger driven enhancement of  
415 upper ocean nutrient supply // Geophysical Research Letters - GEOPHYS  
416 RES LETT. 12 2003. 30.
- 417 Radko Timour, Smith D. Equilibrium transport in double-diffusive convection  
418 // Journal of Fluid Mechanics. 01 2012. 692.
- 419 Ribera d'Alcala Maurizio, Conversano Fabio, Corato Federico, Licandro P.,  
420 Mangoni Olga, Marino D., Mazzocchi Maria Grazia, Modigh M., Montresor  
421 Marina, Nardella M., Saggiomo Vincenzo, Sarno Diana, Zingone Adriana.  
422 Seasonal patterns in plankton communities in pluriannual time series at a  
423 coastal Mediterranean site (Gulf of Naples): An attempt to discern recur-  
424 rences and trends // Scientia Marina. 04 2004. 68. 65–83.
- 425 Ruddick B., Richards K. Oceanic thermohaline intrusions: Observations //  
426 Progress In Oceanography. 03 2003. 56. 499–527.
- 427 Ruddick Barry. A Practical Indicator of the Stability of the Water Column  
428 to Double-Diffusive Activity // Deep Sea Research Part A. Oceanographic  
429 Research Papers. 10 1983. 30. 1105–1107.
- 430 Ruddick Barry, Kerr Oliver. Oceanic thermohaline intrusions: Theory //  
431 Progress In Oceanography. 03 2003. 56. 483–497.
- 432 Schmid Martin, Busbridge Myles, Est Alfred. Double-diffusive convection in  
433 Lake Kivu // Limnology and Oceanography. 01 2010. 55.
- 434 Schmitt Raymond, Ledwell J, Montgomery Ellyn, Polzin K, Toole John. En-  
435 hanced Diapycnal Mixing by Salt Fingers in the Thermocline of the Tropical  
436 Atlantic // Science (New York, N.Y.). 05 2005. 308. 685–8.
- 437 Shibley N., Timmermans M.-L, Carpenter J.R., Toole John. Spatial variability  
438 of the Arctic Ocean's double-diffusive staircase // Journal of Geophysical  
439 Research: Oceans. 02 2017. 122.

440 Stern Melvin. The “Salt-Fountain” and Thermohaline Convection // *Tellus*. 05  
441 1960. 12. 172 – 175.

442 Stommel Henry, Arons Arnold, Blanchard Duncan. An Oceanographical Cu-  
443 riosity, The Perpetual Salt Fountain // *Deep Sea Res.* 01 1956. 3. 152–153.

444 Taillandier Vincent, Prieur Louis, D’Ortenzio Fabrizio, Ribera d’Alcala  
445 Maurizio, Pulido-Villena Elvira. Profiling float observation of thermohaline  
446 staircases in the western Mediterranean Sea and impact on nutrient fluxes //  
447 *Biogeosciences*. 07 2020. 17. 3343–3366.

448 Timmermans Mary-Louise, Garrett Chris, Carmack Eddy. The Thermohaline  
449 Structure and Evolution of the Deep Water in the Canada Basin, Arctic Ocean  
450 // *Deep Sea Research Part I: Oceanographic Research Papers*. 10 2003. 50.

451 Timmermans Mary-Louise, Toole John, Krishfield Richard, Winsor Peter. Ice-  
452 Tethered Profiler observations of the double-diffusive staircase in the Canada  
453 Basin thermocline // *Journal of Geophysical Research*. 12 2008. 113.

454 Turner J. Salt Fingers Across a Density Interface // *Deep Sea Research and*  
455 *Oceanographic Abstracts*. 10 1967. 14. 599–611.

456 *Buoyancy Effects in Fluids*. // . 01 1973.

457 Umlauf Lars, Holtermann Peter, Gillner Christiane, Prien Ralf, Merckelbach  
458 Lucas, Carpenter Jeffrey. Diffusive Convection under Rapidly Varying Con-  
459 ditions // *Journal of Physical Oceanography*. 06 2018. 48.

460 Volosciuk C., Maraun D., Semenov V. A., Tilinina N., Gulev S. K., , Latif M.  
461 Rising Mediterranean Sea Surface Temperatures Amplify Extreme Summer  
462 Precipitation in Central Europe // *Scientific Reports*. 2016. 6, 32450.

463 You Yuzhu. A global ocean climatological atlas of the Turner angle: Implications  
464 for double-diffusion and water-mass structure // *Deep Sea Research Part I:*  
465 *Oceanographic Research Papers*. 11 2002. 49. 2075–2093.

466 Zhang Jubao, Schmitt Raymond, Huang Rui. Sensitivity of the GFDL Modular  
467 Ocean Model to Parameterization of Double-Diffusive Processes // *Journal*  
468 *of Physical Oceanography - J PHYS OCEANOGR*. 04 1998. 28. 589–605.

469 Zingone Adriana, Casotti Raffaella, Ribera d’Alcala Maurizio, Scardi Michele,  
470 Marino Donato. St-Martin’s Summer - The case of an Autumn phytoplankton  
471 bloom in the Gulf of Naples (Mediterranean-Sea) // *Journal of Plankton*  
472 *Research*. 03 1995. 17. 575–593.

473 Zingone Adriana, D’Alelio Domenico, Mazzocchi Maria Grazia, Montresor  
474 Marina, Sarno Diana. Time series and beyond: Multifaceted plankton re-  
475 search at a marine Mediterranean LTER site // *Nature Conservation*. 05  
476 2019. 34. 273–310.

- 477 Zingone Adriana, Dubroca Laurent, Iudicone Daniele, Margiotta Francesca,  
478 Corato Federico, Ribera d'Alcala Maurizio, Saggiomo Vincenzo, Sarno Diana.  
479 Coastal Phytoplankton Do Not Rest in Winter // Estuaries and Coasts. 03  
480 2010. 33. 342-361.
- 481 Zodiatis George, Gasparini Gian. Thermohaline staircase formations in the  
482 Tyrrhenian Sea // Deep-sea Research Part I-oceanographic Research Papers  
483 - DEEP-SEA RES PT I-OCEANOGRAPHIC RES. 05 1996. 43. 655-678.

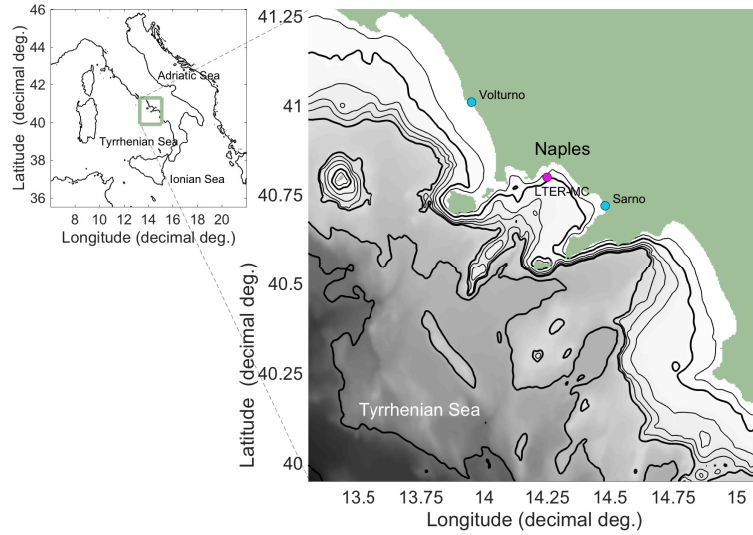


Figure 1: Bathymetry of the Gulf of Naples (GEBCO grid (GEBCO, 2020)) along the Tyrrhenian Sea in the Mediterranean basin). The 75m-deep LTER-MC coastal sampling site ( $14.25^{\circ}E, 40.80^{\circ}N$ ) is located by the pink dot. Volturno and Sarno's river mouths are shown in blue. Thin lines indicate the 50, 200, 300 and 400 m isobaths, thick ones indicate the 100, 500, 1000 and 2000 m isobaths.

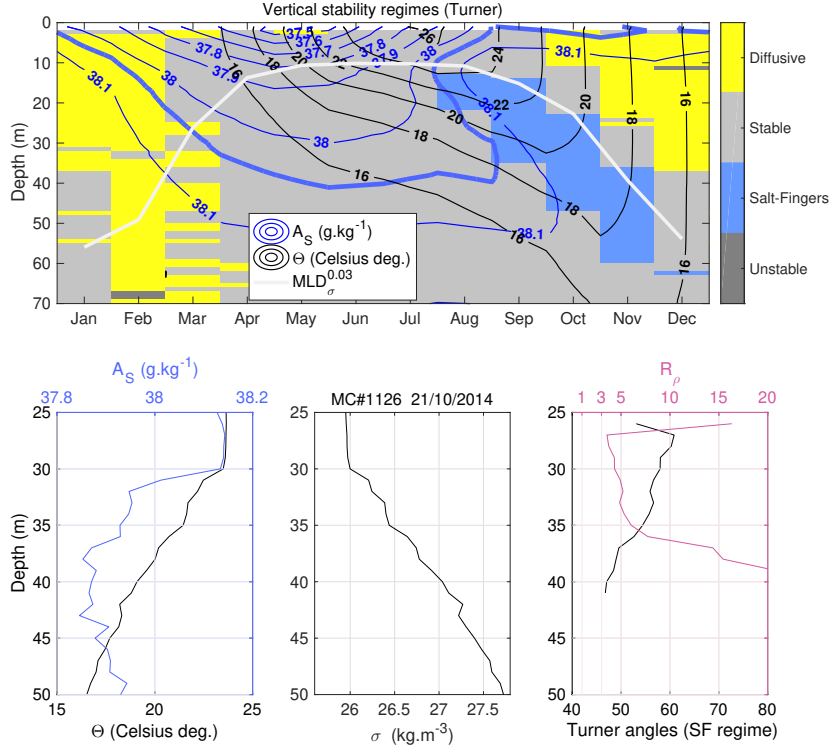


Figure 2: **Top** : Seasonal water-column occupation by the four stability regimes of Turner, showing vertical layers prompt to possibly host double-diffusive instabilities (SF or DDF), inferred from the monthly climatological profiles established with the weekly CTD data from 2001 to 2020 (MC465 to MC1359). Black and blue : contours of the climatological temperature and salinity profiles. Thick blue :  $38.05 \text{ g kg}^{-1}$  haline level, showing the salty intrusion. Light gray : seasonal mixed layer depth (MLD). **Bottom** : Illustration of a density staircase situation (cast MC1126). Left : temperature and salinity profiles ; Center : density ; Right : Turner angles and density ratio  $R_\rho$  (SF regime).

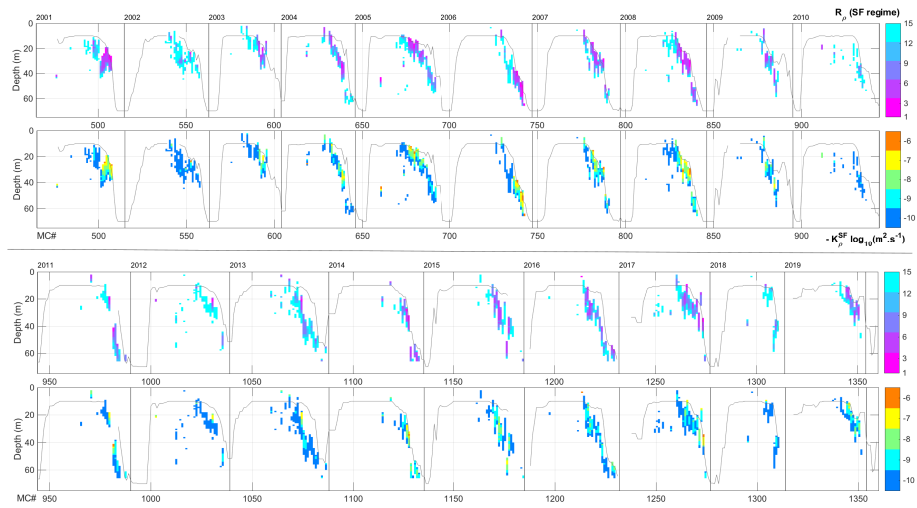


Figure 3: Time series of the vertical profiles of  $R_\rho$  (pink to light blue chart, on Top) and the effective eddy diffusivity  $K_\rho$  (blue to orange chart, on Bottom), for the SF regime. Decades are splitted between upper (2001-2010) and lower (2011-2020) panels. Y-axis indicates the depth of profiles, x-axis indicates the sequence of weekly MC casts (MC465 to MC1359). Years are indicated at the top. Gray line : mixed layer depth.

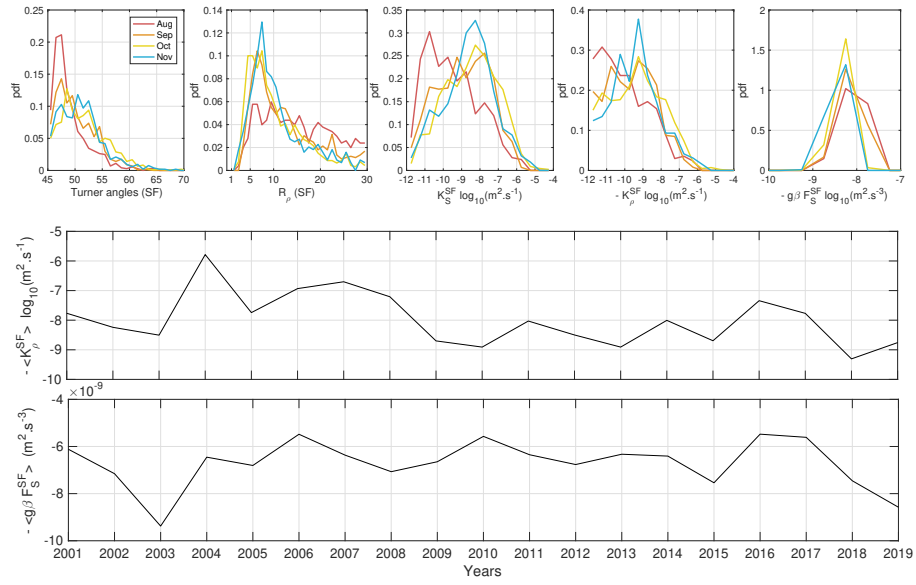


Figure 4: **Top** : Probability density function (PDF) associated with the following parameters in the SF regime : Turner angles,  $R_\rho$ , effective salt diffusivity ( $K_S$ ), effective eddy diffusivity ( $K_\rho$ ), and buoyancy flux for salt. Distributions have been established from the whole period available (2001 to 2020), and separated for the four month of August to November when SF regime is possible. **Bottom** : Inter-annual variability of the year-averaged mean values of  $K_\rho^{\text{SF}}$  and buoyancy flux for salt  $g\beta F_S^{\text{SF}}$  (note the negative values).